Experimental Investigation of Two Bio-inspired MPPT Algorithms for Partially Shaded PV Arrays

Abd-Elwahab Khalifa, Medhat H. Elfar, Qays Adnan Ali, Ahmed Elbaz, Ahmed Kalas, Mohamed Mohamed Elsakka, Nikolay V. Korovkin, and Ahmed Refaat

1 Introduction

The use of renewable energy resources (RERs) has been increasing around the world in recent decades due to concerns about carbon footprint and energy shortages. The most promising RER technology of the twenty-first century is solar photovoltaic (PV) energy since it has some advantages such as green energy, low operating cost, zero carbon emission, zero fuel consumption, low maintenance cost, low noise pollution, and can be established to any size depending on the energy requirements. However, it suffers from a considerably high capital cost and low energy efficiency. Therefore,

A.-E. Khalifa · M. H. Elfar · A. Elbaz · A. Kalas · A. Refaat (✉)
Department of Electrical Engineering, Faculty of Engineering, Port Said University, Port Said, Egypt
e-mail: ahmed_refaat_1984@eng.psu.edu.eg

M. H. Elfar
e-mail: mhelfar@eng.psu.edu.eg

A. Elbaz
e-mail: ahmed.sabry@eng.psu.edu.eg

A. Kalas
e-mail: ahmed.kalas@eng.psu.edu.eg

Q. A. Ali
Department of Fuel and Energy Techniques Engineering, Technical Engineering College, Northern Technical University, Kirkuk, Iraq
e-mail: alnajarqays@ntu.edu.iq

M. M. Elsakka
Department of Mechanical Power Engineering, Faculty of Engineering, Port Said University, Port Said, Egypt

Energy Research and Studies Unit, Faculty of Engineering, Port Said University, Port Said, Egypt

A. M. Negm et al. (eds.), *Engineering Solutions Toward Sustainable Development*, Earth and Environmental Sciences Library, https://doi.org/10.1007/978-3-031-46491-1_6

it is crucial to optimize the power generated from PV systems by utilizing suitable control schemes [1–6].

The key challenge for capturing the maximum power from the outdoor PV systems is the uneven fallen of solar irradiation on the upper surface of the PV array owing to the partial shading conditions (PSCs). The PSCs lead to the distortion of the P–V characteristic curves of the PV array where multiple peaks are emerged including one global peak (GP) beside one or more local peaks (LPs). Indeed, the connection of the bypass protective diodes across each panel in the PV array is the main reason for these distortions in the P–V curves. However, bypass protective diodes are mandatory in PV system installations to protect the PV panels that may be destroyed under the PSCs due to the hot-spot phenomenon [7, 8].

Classical algorithms-based-maximum power point tracking (MPPT) controllers such as incremental conductance (InC), perturb and observe (P&O), and their improved versions have been suggested in the literature [9–12]. Classical algorithms have relatively simple structures, easy to executions, and a low computation burden. Nevertheless, these algorithms suffer from a trade-off between tracking speed and tracking accuracy. For instance, if the step size in the algorithm is increased to obtain fast-tracking time, high steady-state power oscillations are observed that lead to low tracking accuracy. On the other hand, if the step size in the algorithm is reduced to acquire relatively low steady-state power oscillations, the convergence speed of the algorithms is slowed down resulting in a high tracking time. In addition, these algorithms are frequently trapped in LPs under the PSCs [13–15].

Recently, AI techniques are widely employed in the MPPT controllers for PV systems in order to guarantee the successful tracking of the GPs under the PSCs [16]. Many AI-based approaches have been introduced in the literature including Fuzzy Logic Control-based MPPT controllers [17], Deep Learning Techniques-based MPPT controllers, and Bio-inspired Algorithms-based MPPT controllers. Numerous bio-inspired algorithms have been developed by researchers to address the PSCs problems such as Ant-Lion Optimization (ALO) [18], Grasshopper Optimization (GHO) [19], Cuckoo Search (CS) [20], Search and Rescue Algorithm (SRA) [21], Bat Algorithm (BA) [22], Grey Wolf Optimization (GWO) [23], Sine Cosine Algorithm (SCA) [24], Yellow Saddle Goatfish Algorithm (YSGA) [25], Firefly Algorithm (FA) [26], Moth-Flame Optimization (MFO) [27], Earthquake Algorithm (EA) [28], Flower Pollination Algorithm (FPA) [29], Dragonfly Optimization Algorithm (DFOA) [30], Harris Hawk Optimization Algorithm (HHOA) [31], Hybrid Particle Swarm Optimization-Fireworks (PSO-FW) algorithm [32], Salp-Swarm Optimization Algorithm (SSOA) [33], Artificial Bee Colony (ABC) algorithm [34], Group Teaching Optimization Algorithm (GTOA) [35], and others.

M. M. Elsakka
e-mail: Elsakka@eng.psu.edu.eg

N. V. Korovkin
Institute of Energy, Peter the Great Saint Petersburg Polytechnic University, Saint Petersburg, Russia

This article introduces a comparative study between the performance of the Autonomous Group Particle Swarm Optimization (AGPSO) algorithm and the Cuckoo Search (CS) algorithm for partially shaded photovoltaic (PV) arrays. Firstly, the performance of the two algorithms is assessed under different weather conditions including STC and PSCs by using MATLAB/SIMULINK. Then, an experimental study is conducted to validate the obtained simulation results.

2 System Configuration

The entire PV system configuration is depicted in Fig. 1. The PV system under study composed of four main parts, including the PV array, power conditioning unit, load, and maximum power point tracking (MPPT) controller. A 450 W PV array is constructed by three parallel strings, each string consists of three series-connected PV panels. The PV panel produces a maximum power of about 50.04 W with a MPP voltage of 19.01 V and a MPP current of 3.16 A at the standard test conditions $\left(STC: T_{ref} = 25\,°\mathrm{C}, G_{ref} = 1000\,\mathrm{W/m^2}\right)$. A 50 Ω resistive load is interfaced with the PV array through a boost converter. The specifications of the boost converter design to work in continuous conduction mode have been listed in Table 1. The MPPT controller continually monitors the PV array power using current and voltage sensors and then regulates the duty cycle of the boost converter to assure that it operates at its MPP under various weather conditions. This ensures that maximum power is extracted from the PV array and delivered to the load.

In order to study the impact of weather conditions on the PV system performance, several mathematical models based on the equivalent circuits have been proposed in the literature [36]. A typical representation of the PV cell using a five-parameter model is illustrated in Fig. 2. This model presents an excellent balance between model complexity and accurateness, and its parameters $(I_{Ph}, I_0, R_{sh}, R_s, m)$ are numerically determined in accordance with previous literature [36].

The fundamental equations describing the characteristics of the PV array model taking into consideration the effect of solar radiation change and cells operating temperature are as follows:

$$\begin{aligned} I_{PV} &= I_{Ph} N_{pr} \\ &\quad - I_0 N_{pr} \left\{ \exp\left[\frac{V_{PV} + I_{PV} R_s \left(\frac{N_{sr}}{N_{pr}}\right)}{m V_t N_{sr}} \right] - 1 \right\} - \frac{V_{PV} + I_{PV} R_s \left(\frac{N_{sr}}{N_{pr}}\right)}{R_{sh} \left(\frac{N_{sr}}{N_{pr}}\right)} \end{aligned} \tag{1}$$

$$I_{Ph} = \left[I_{Ph,T_{ref}} + \alpha_I \left(T_c - T_{ref}\right) \right] \left(\frac{G}{G_{ref}} \right) \tag{2}$$

$$I_{Ph,T_{ref}} = \frac{R_{sh} + R_s}{R_{sh}} I_{sc,T_{ref}} \tag{3}$$

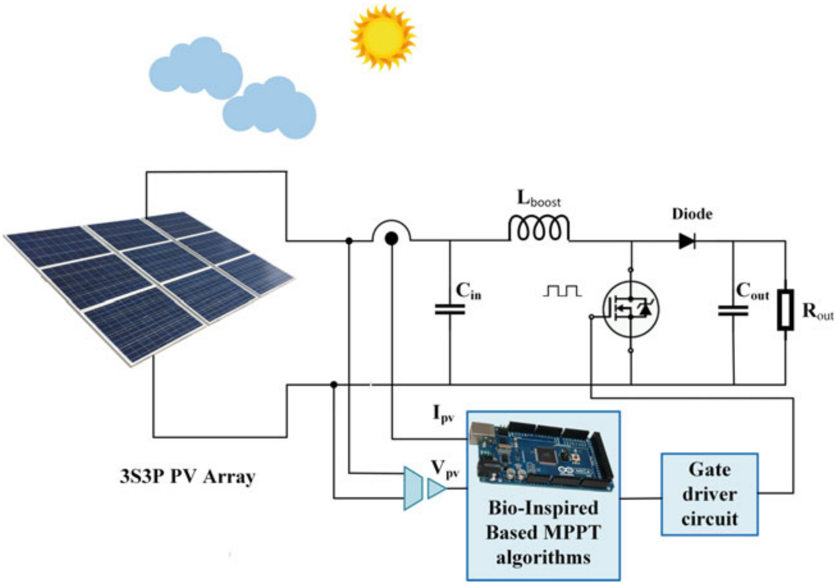

Fig. 1 The system configuration

Table 1 Specifications of boost converter

Component	Value
Input capacitor	100 μF
Output capacitor	500 μF
Boost inductor	1.5 mH
Switching frequency	10 kHz

Fig. 2 Equivalent circuit of the five-parameter model of a PV cell

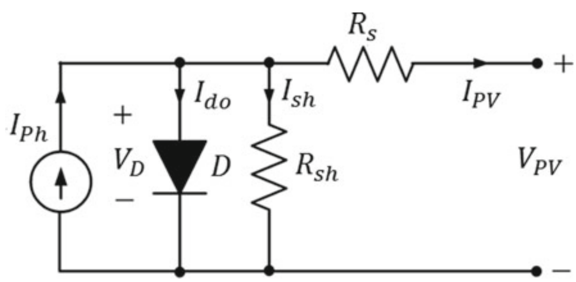

$$I_0 = \frac{I_{sc,T_{ref}} + \alpha_I\left(T_c - T_{ref}\right)}{\left\{\exp\left(\frac{V_{oc,T_{ref}} + \alpha_V\left(T_c - T_{ref}\right)}{mV_t}\right) - 1\right\}} \tag{4}$$

where I_{PV} denotes the array output current, V_{PV} denotes the array output voltage I_{Ph} denotes the photo-current, I_0 is the dark saturation current, q is the electron charge, N_{sr} is No. of series-connected panels, N_{pr} is the No. of parallel-connected strings, ($v_t = n_s K T_c / q$) is the panel thermal voltage, K denotes the Boltzmann constant, T_c is the panel temperature, m denotes the diode ideality factor $I_{Ph,T_{ref}}$ is the photo-current at STC, $V_{oc,T_{ref}}$ refers to the open-circuit voltage at STC, $I_{sc,T_{ref}}$ refers to the short circuit current at STC, α_V and α_I are the voltage and current temperature coefficients, respectively.

3 Bio-Inspired Optimization Algorithms

Bio-inspired techniques use algorithms that mimic natural processes such as genetic algorithms, neural networks, and swarm intelligence. These algorithms permit a more efficient and effective optimization process than traditional methods. In this article, the Autonomous Group Particle Swarm Optimization (AGPSO) algorithm and the Cuckoo Search (CS) algorithm are utilized to acquire the optimum duty cycle under different environmental conditions. This section provides an overview of the AGPSO and CS algorithms including the mechanism of operation, the mathematical model, and the MPPT flowchart for each algorithm.

3.1 AGPSO Algorithm

Particle Swarm Optimization (PSO) algorithm is widely utilized in various applications because of its simple structure, ease of establishment, and low computational cost. The PSO algorithm, however, has some drawbacks for MPPT applications, such as the challenge of adjusting its parameters under various environmental conditions, long convergence time, and the possibility of being trapped in LP under PSCs [37]. In order to tackle the issues related to the PSO algorithm, AGPSO algorithm is employed in this study.

Balancing between the exploration and exploitation phases during the search process is the main challenge for the classical PSO algorithm. The search behavior of particles in the search space for the PSO algorithm is dependent on the value of the cognitive and social parameters (c_1 and c_2). The particles have a high ability for local exploration throughout the search process if the cognitive parameter c_1 is relatively higher than the social parameter c_2. Conversely, if the parameter c_2 is relatively greater than c_1, then the particles search more globally, and exploit information compiled to converge towards the optimal solution [38].

The AGPSO is a bio-inspired algorithm that mimics the behavior of termite colonies in nature. Particles in a classical PSO algorithm may be considered as a group with a single strategy since all particles exhibit the same behavior in terms of local and global search. On the other hand, the particles in the AGPSO algorithm are separated into four independent groups, each of which has a different strategy for searching both locally and globally. This led to the improvement of the algorithm performance since a better equilibrium between the exploration and exploitation phases is achieved during the search process [39].

In the AGPSO algorithm, the acceleration parameters are modeled by employing third root and cubic functions instead of using constant parameters as in classical PSO. These functions are chosen with various curvatures, intersection points, and slopes as shown in Fig. 3. The updating strategy of c_1 and c_2 for each group is provided in Table 2. In this work, the inertial weight parameter is decreased linearly from 0.9 to 0.4 as given in Eq. (5). Using the AGPSO algorithm as an MPPT controller, the mathematical equations to update the duty cycle of the DC–DC boost converter and its step size are as follows:

$$\omega^k = \omega_{\max} - (\omega_{\max} - \omega_{Min}).{}^{k}\!/_{k_{\max}} \tag{5}$$

$$\Delta D_i^{k+1} = \omega^k.\Delta D_i^k + c_1.r_1.\left(D_{Pbest} - D_i^k\right) + c_2.r_2\left(D_{Gbest} - D_i^k\right) \tag{6}$$

$$D_i^{k+1} = D_i^k + \Delta D_i^{k+1} \tag{7}$$

where k is the No. of iteration, i denotes the No. of particles, ω^k is value of the inertia weight at the iteration k, $\omega_{\max} = 0.9$ and $\omega_{\min} = 0.4$ are the upper and lower bounds of ω^k, D^i denotes the duty cycle of the i th-particle, ΔD_i is the perturbation step, c_1 and c_2 are the acceleration coefficients, r_1 and r_2 are random numbers $\in$ [0, 1] denotes the personal best position of the i th-particle, and D_{Gbest} is the global best position. The flow chart of the AGPSO MPPT algorithm is depicted in Fig. 4.

3.2 CS Algorithm

CS is a bio-inspired algorithm created by Xin-She Yang et. al in 2009 [40]. It is inspired by the parasitic behavior of cuckoo birds (CBs), which lay their eggs in the nests of other host birds instead of constructing their own nest as shown in Fig. 5. The CBs move around randomly, but they are also guided by an exploration–exploitation mechanism that encourages them to explore new nests in the search space while also exploiting promising nests they have already discovered.

The exploration–exploitation mechanism works by evaluating each cuckoo's current position in the search space and assigning it a fitness value based on how close it is to the optimal solution. The cuckoos with higher fitness values are more likely to be chosen for reproduction, while those with lower fitness values are more likely to be replaced by new cuckoos generated from random positions in the search space.

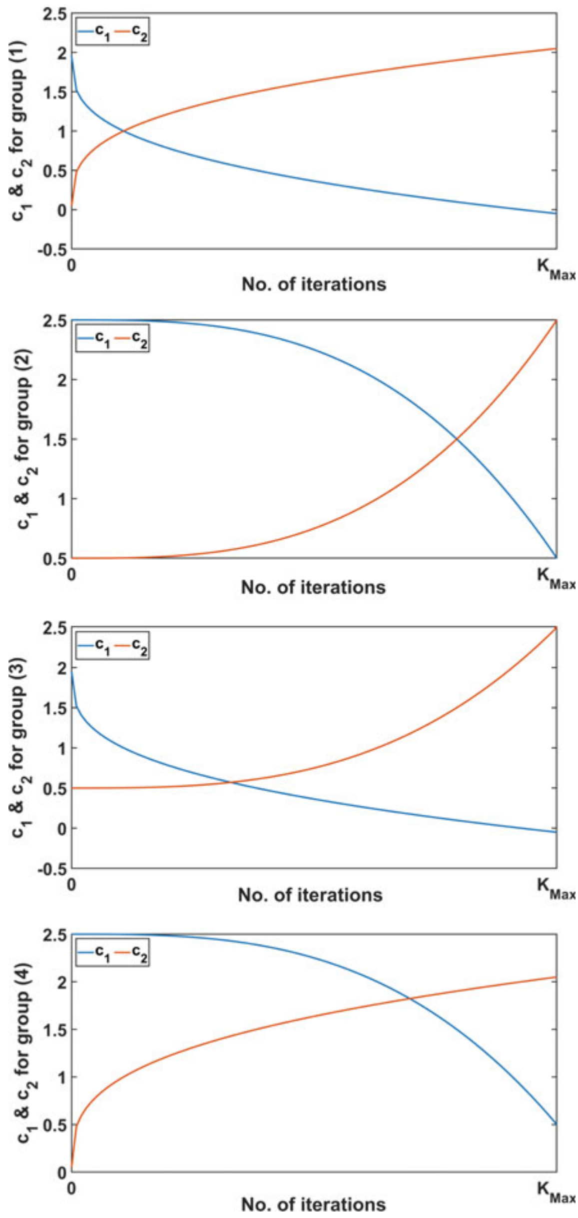

Fig. 3 The updating values of c1 and c2 for the four groups utilized in the AGPSO algorithm

This process continues until the optimal solution is found or until all possible solutions have been explored. Hence, the CBs improve their opportunities of surviving by placing their eggs in numerous nests.

The reproduction behavior of the CBs is employed in the CS algorithm. Random movements based on the Lévy flight function enable CB a long jump in the search

Table 2 The updating strategies for c_1 and c_2

Group No.	Updating of c_1	Updating of c_2
(1)	$1.95 - \left(2k^{1/3}/k_{\text{Max}}^{1/3}\right)$	$\left(2k^{1/3}/k_{\text{Max}}^{1/3}\right) + 0.05$
(2)	$\left(-2k^{3}/k_{\text{Max}}^{3}\right) + 2.5$	$\left(2k^{3}/k_{\text{Max}}^{3}\right) + 0.5$
(3)	$1.95 - \left(2k^{1/3}/k_{\text{Max}}^{1/3}\right)$	$\left(2k^{3}/k_{\text{Max}}^{3}\right) + 0.5$
(4)	$\left(-2k^{3}/k_{\text{Max}}^{3}\right) + 2.5$	$\left(2k^{1/3}/k_{\text{Max}}^{1/3}\right) + 0.05$

space which enhances the algorithm performance and increases its convergence speed. The flow chart of the CS algorithm to obtain the optimal duty cycle for the MPPT controller of the PV system is depicted in Fig. 6. The following mathematical model is utilized to construct the algorithm.

$$D_i^{k+1} = D_i^k + \alpha \oplus L\acute{e}vy(\lambda) \tag{8}$$

$$L\acute{e}vy(\lambda) \approx \mathcal{X}\left(\frac{u}{|v|^{\frac{1}{\beta}}}\right)(D_{best} - D_i) \tag{9}$$

$$v \approx N\left(0, \sigma_v^2\right) \text{ and } u \approx N\left(0, \sigma_u^2\right) \tag{10}$$

$$\sigma_u = \left(\frac{\Gamma(1+\beta) \times \sin\left(\frac{\pi\beta}{2}\right)}{\Gamma\left(\frac{1+\beta}{2}\right) \times \beta \times 2^{\left(\frac{\beta-1}{2}\right)}}\right)^{\frac{1}{\beta}} \tag{11}$$

$$\sigma_v = 1 \tag{12}$$

where α is a scaling factor to adjust the step size, $L\acute{e}vy$ refer to the levy flights, λ is the variance, D_{best} denotes of the best duty cycle, Γ denotes the gamma function $\mathcal{X}$ denotes Lévy multiplication coefficient, $\beta = 1.5$ and u and v are calculated from the normal distribution curves.

4 Simulation Results

In order to evaluate the performance of both algorithms for MPPT application, the PV system in Fig. 1 has been carried out on MATLAB/SIMULINK. Four cases of weather conditions have been chosen to assess the performance of each algorithm in terms of tracking accuracy and speed. The pattern of the fallen solar irradiance on the surface of the PV array is presented in Table 3, and the associated P–V characteristic

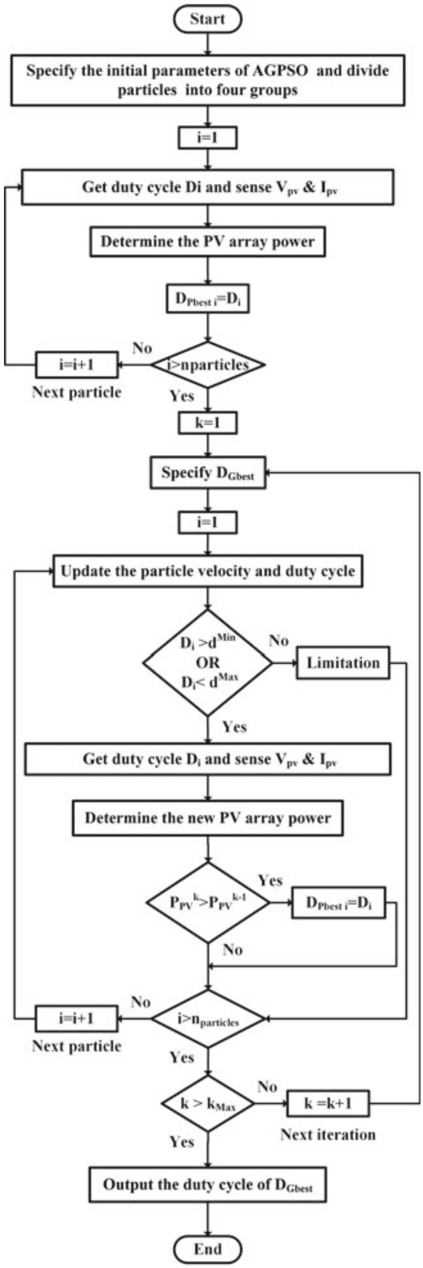

Fig. 4 Flowchart of the MPPT based on the AGPSO algorithm

Fig. 5 The reproductive behavior of the CBs in nature

of the PV array for each case are shown in Fig. 7. Each case has a different MPP voltage and MPP power with a different curvature on the P–V characteristic. The first case handles the STCs which have a unique MPP, whereas the remaining cases address three dissimilar PSCs which have several MPPs. The three shaded patterns are more challenging for the MPPT controller since it must discriminate the GP among the other LPs to harvest the maximum power available.

The output power and duty cycle of both methods for considered weather patterns are illustrated in Figs. 8, 9, 10 and 11. The acquired power, tracking time, and MPPT efficiency for both techniques have been listed in Table 4. As shown, the maximum power that should be harvested for the GP1, GP2, GP3, and GP4 is 450.36 W, 149.98 W, 194.3 W, and 296.27 W, respectively.

Regarding the first case, the obtained numerical results of the PV system for both controllers under STCs are depicted in Fig. 8. As illustrated, CS and AGPSO algorithms have a maximum power of 449.25 W and 449.35 W with a tracking time of 0.163 s and 0.297 s, respectively. This indicates that the utilization of the CS algorithm reduces the tracking time by almost 82%. Furthermore, the CS algorithm has more tracking accuracy with an MPPT efficiency of 99.78% compared to 99.75% for the AGPSO algorithm.

Under the PSCs, three shaded patterns have been selected with different GP location on the P–V curve, particularly case 2, case 3, and case 4 that are corresponding to GP location at the left, middle, and right relative to the other MPPs; respectively,

Fig. 6 Flowchart of the MPPT based on the CS algorithm

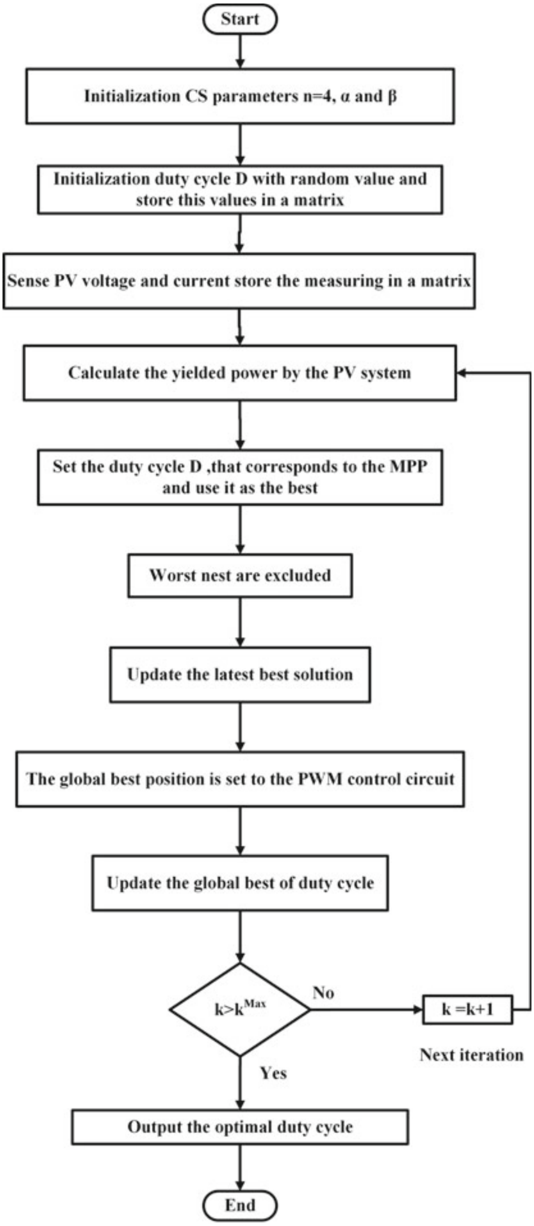

Table 3 The pattern of the fallen solar irradiance on the regarded PV array

Shading pattern	Solar irradiance (kW/m^2)		
Case 1	1.0	1.0	1.0
	1.0	1.0	1.0
	1.0	1.0	1.0
Case 2	1.0	1.0	1.0
	0.3	0.3	0.3
	0.2	0.2	0.2
Case 3	1.0	1.0	1.0
	0.6	0.6	0.6
	0.2	0.2	0.2
Case 4	1.0	1.0	1.0
	0.8	0.8	0.8
	0.6	0.6	0.6

as shown in Fig. 7. Simulation results show that the CS algorithm has a better performance than the AGPSO algorithm under all tested PSCs as demonstrated in Table 4. The reduction in the convergence time for GP_2, GP_3, and GP_4 is about 47.36%, 47%, and 60%, respectively. In addition, the CS algorithm has a higher tracking accuracy with MPPT efficiencies of 99.94%, 99.79%, and 99.84% in contrast with the AGPSO algorithm which has MPPT efficiencies of 99.93%, 99.52%, and 99.67% for GP_2, GP_3, and GP_4, respectively.

5 Experimental Results

In this section, experimental studies are conducted in order to validate the simulation results for both considered algorithms-based controllers under the PSCs. The experimental tests had been carried out on the selected PV testing site which is equipped with a pyranometer and provides easy access to the nearby solar energy laboratory. The selected test site is located on the roof of the teaching building in the Faculty of Engineering at Port Said. The exact location of the PV testing site is identified with Latitude: 31° 14′ 50.97" N and longitude: 32° 18′ 44.63" E. Figure 12 shows the experimental hardware setup for the considered PV system. The 3S3P PV array is mounted at a fixed tilt angle of 30° facing south. The PV panel temperature is measured by a thermocouple installed on the back surface of each panel. The shading pattern is constructed by employing opaque and semi-transparent sheets as depicted in Fig. 12. A data logger records the data about the weather condition to acquire the P–V curve of the PV array under the tested PSC.

The PV array is connected to the load via the boost converter. The specifications of the designed converter are $f_{sw} = 31.372$ kHz, $L_{boost} = 2.6$ mH, $C_{in} = 330\,\mu F$, and $C_{out} = 1000\,\mu F$. Two measurement circuits have been implemented to monitor

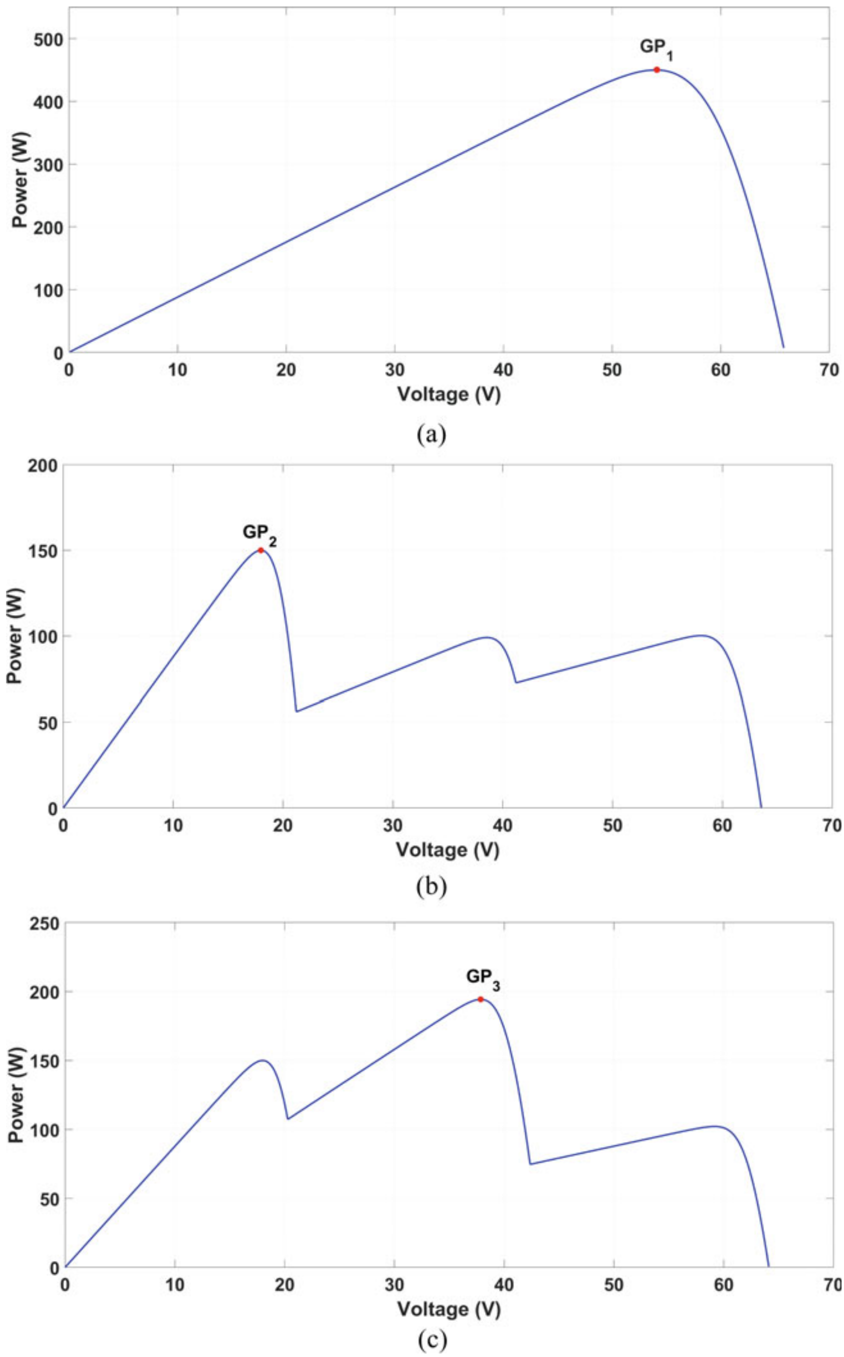

Fig. 7 The P–V curves of the PV array for various weather conditions: **a** case 1, **b** case 2, **c** case 3, and **d** case 4

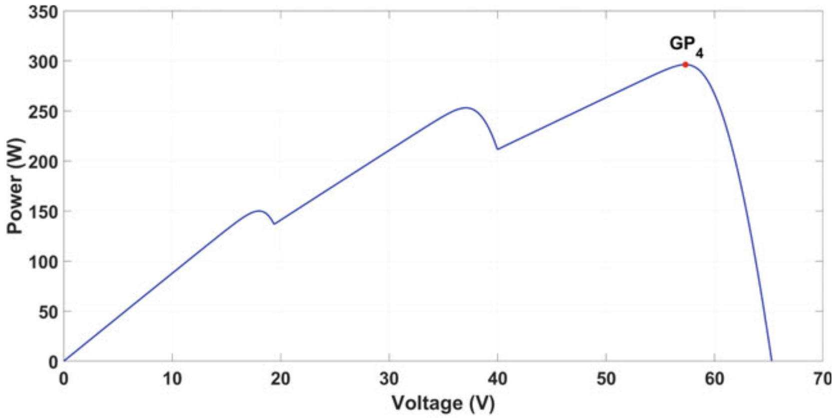

(d)

Fig. 7 (continued)

the output of the PV array and the load. The input sensors measure the array current and voltage and send the sensed signals to the controller. Arduino Mega 2560 is used in this study which is interfaced with MATLAB through a supported package. The tested algorithms are deployed on the controller that generates the optimal duty cycle and then sent its value to the TLP250 drive circuit. A digital oscilloscope has been employed to display the PWM signal.

The obtained P–V characteristic for experimental studies is illustrated in Fig. 13. As it is noticed, the characteristic curve displays numerous MPPs with the GP on the right side of the curve. The value of the power and voltage for the GP is 158.3 W and 54.53 V. The corresponding experimental results of the PV array power and voltage for the two algorithms are shown in Figs. 14 and 15. As can be seen from Fig. 14, the AGPSO algorithm reached a maximum power of about 155.72 W at an MPP voltage of 53.85 V and tracking efficiency of about 98.4%. It has an MPPT time of about 5 s with high power fluctuations of about 4.7 W at steady-state conditions. On the other hand, the CS algorithm has a maximum power of almost 156.02 W at an MPP voltage of 53.91 V and tracking efficiency of about 98.6% as shown in Fig. 15. It reached the MPP in just 2.9 s with lower power fluctuations of about 3.4 W at steady-state conditions. Overall, the experimental results indicate that the performance of the CS algorithm is better than the AGPSO algorithm in terms of tracking accuracy and speed.

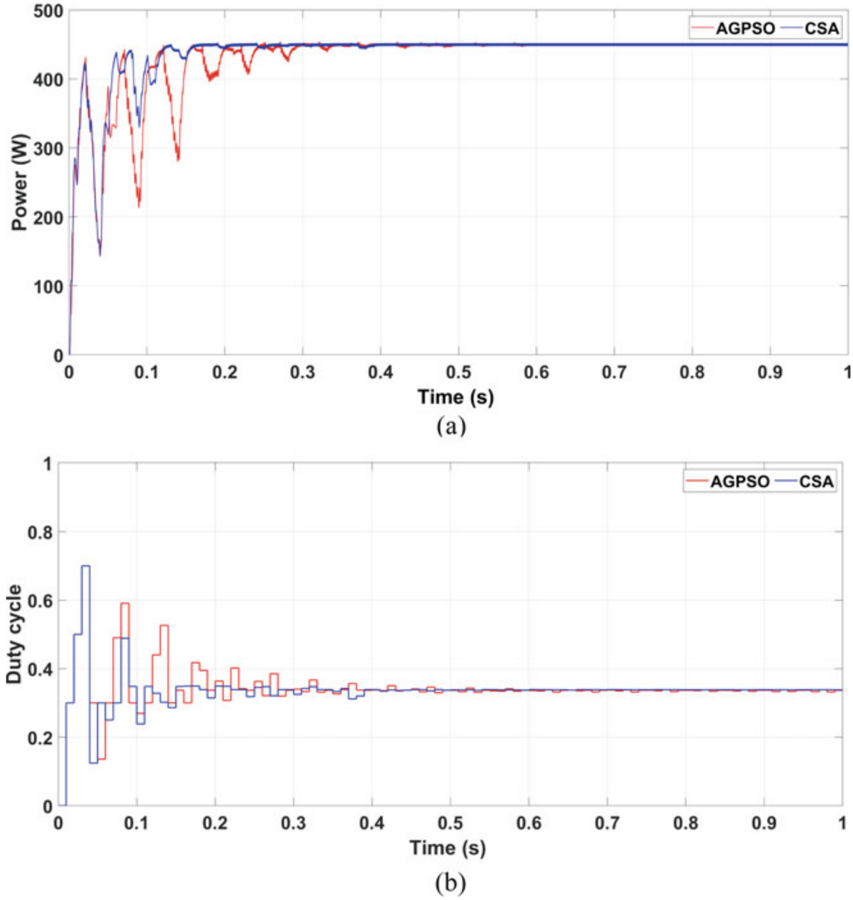

Fig. 8 The behavior of both algorithms for case 1: **a** output power and **b** duty cycle

6 Conclusion

This article presented a comprehensive comparison between AGPSO and CS algorithms for harvesting the maximum power from the PV system under the PSCs. The mechanism of operation, the mathematical model, and the MPPT flowchart for both considered bio-inspired algorithms were explained. MATLAB simulations and experimental tests were carried out to compare both algorithms' performance under various weather conditions.

From the obtained results, the two bio-inspired algorithms can follow the GP of the PV array under tested conditions with low convergence time and high MPPT accuracy. Although the AGPSO algorithm can successfully trace the GP, the CS algorithm outperforms it with a higher convergence speed and tracking accuracy. The simulation results demonstrated that using the CS algorithm decreased the MPPT time by 82%,

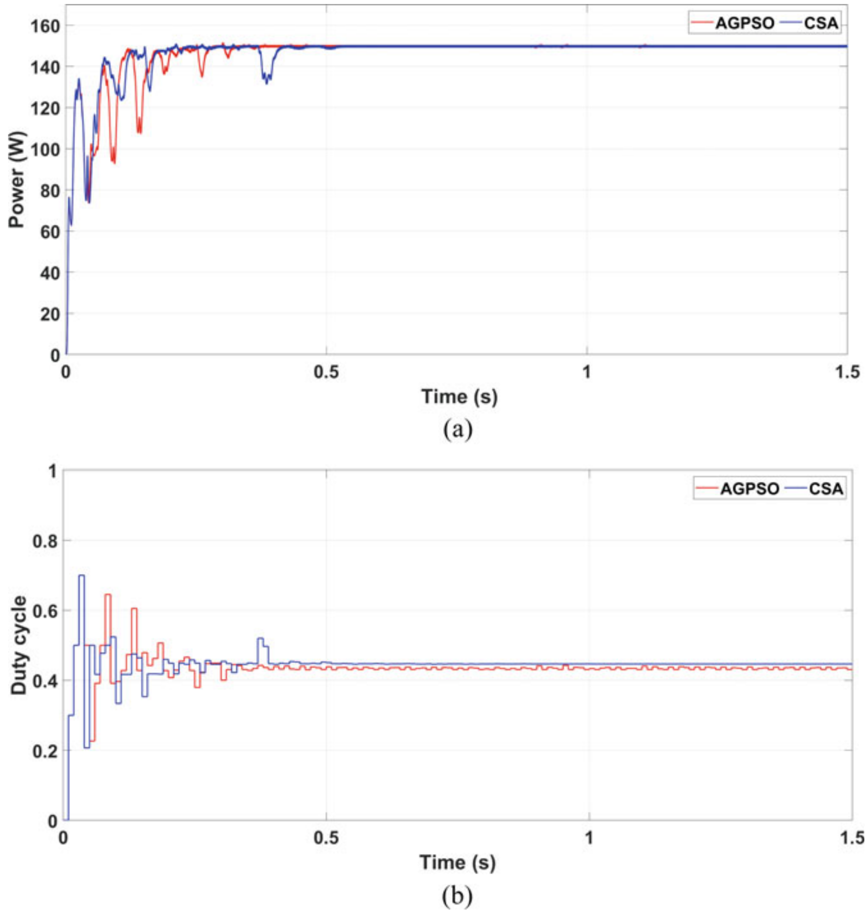

Fig. 9 The behavior of both algorithms for case 2: **a** output power and **b** duty cycle

47.36%, 47%, and 60% for GP_1, GP_2, GP_3, and GP_4, respectively. Furthermore, the tracking efficiency for the CS algorithm was higher than the AGPSO algorithm under various weather patterns. Experimental results confirmed the simulation results since the tracking time of the CS algorithm was reduced by almost 42% compared with the AGPSO algorithm. In addition, the CS algorithm was found to have lower power fluctuations and higher MPPT accuracy than the AGPSO algorithm counterpart.

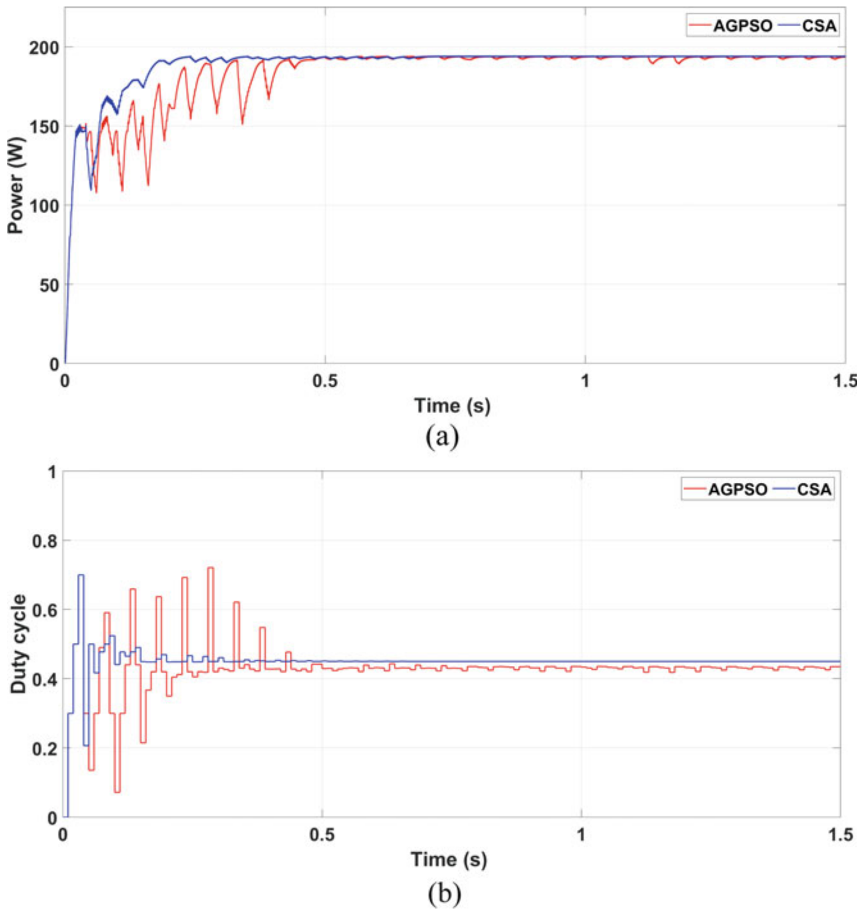

Fig. 10 The behavior of both algorithms for case 3: **a** output power and **b** duty cycle

7 Recommendation

Based on the previous findings, it is recommended to carry out a bio-inspired-based-MPPT algorithm in PV systems to extract the maximum power from PV systems under PSCs and hence improve the system efficiency. This enhances the endeavors of fulfilling SDG 7: Affordable and clean energy through optimizing the energy harvest from PV systems.

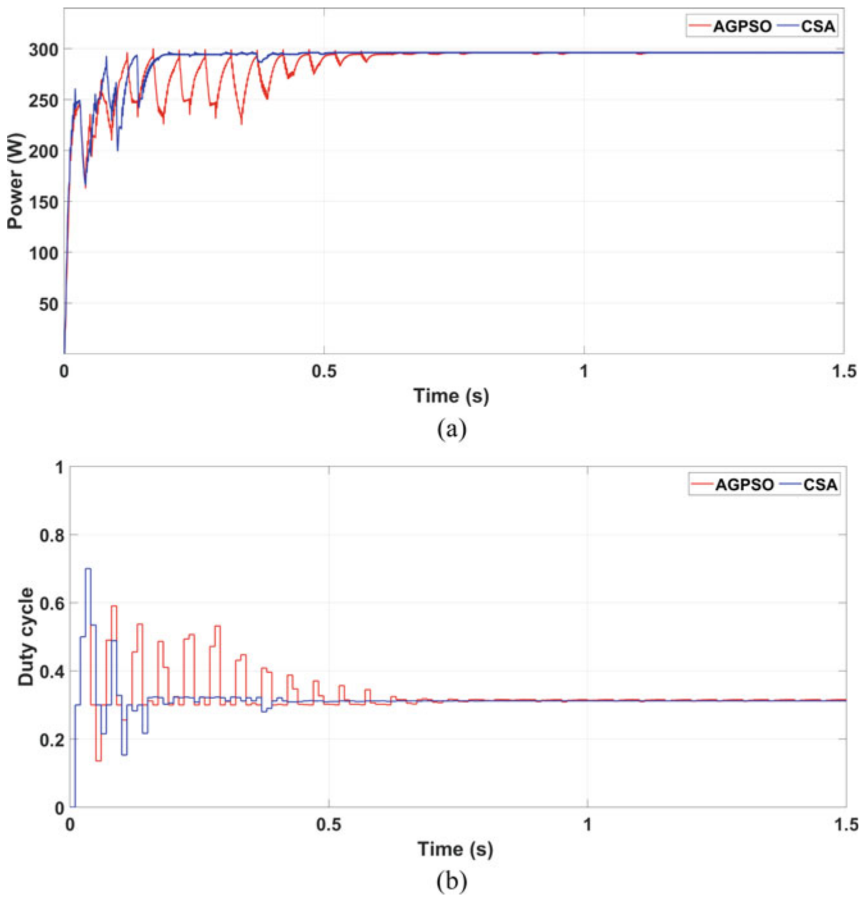

Fig. 11 The behavior of both algorithms for case 4: **a** output power and **b** duty cycle

Table 4 Performance of bio-inspired algorithms for different patterns of solar radiation

Pattern	Algorithm	Power (w)	Tracking time (s)	GP power (w)	MPPT Efficiency (%)
Case 1	AGPSO	449.25	0.297	450.36	99.75
	CS	449.35	0.163		99.78
Case 2	AGPSO	149.87	0.283	149.98	99.93
	CS	149.89	0.199		99.94
Case 3	AGPSO	193.36	0.494	194.3	99.52
	CS	193.9	0.336		99.79
Case 4	AGPSO	295.3	0.596	296.27	99.67
	CS	295.8	0.202		99.84

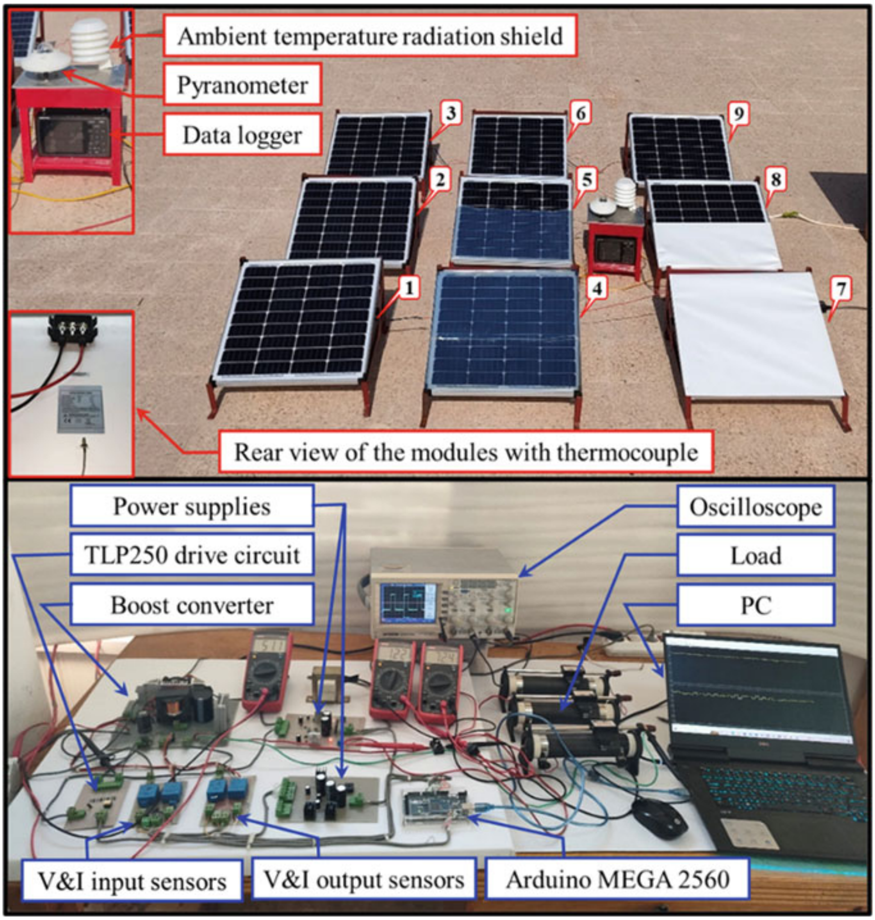

Fig. 12 Experimental hardware setup for the considered PV system

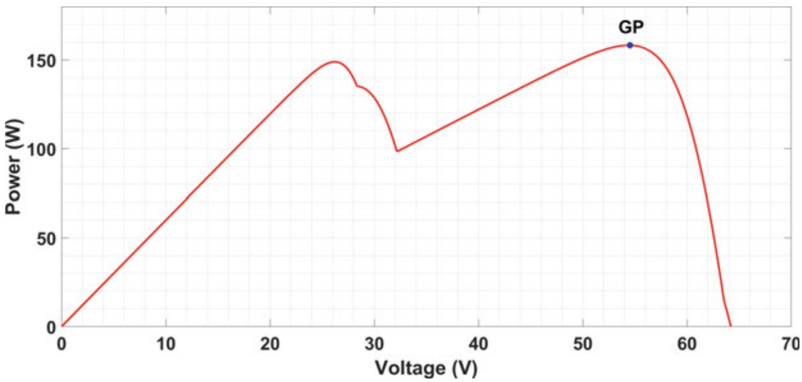

Fig. 13 The acquired P–V curve for the experimental test

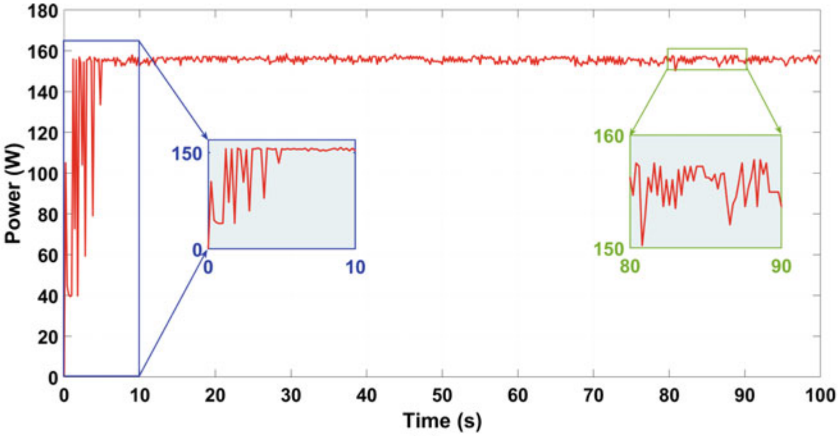

(a)

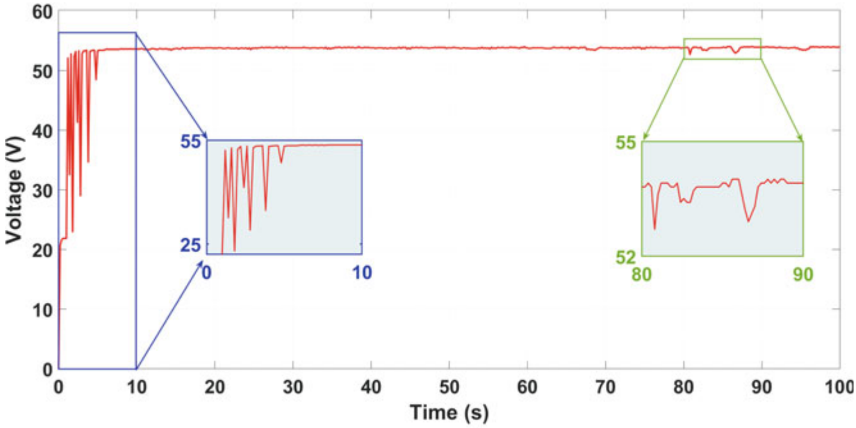

(b)

Fig. 14 Experimental results for the AGPSO algorithm: **a** power and **b** voltage

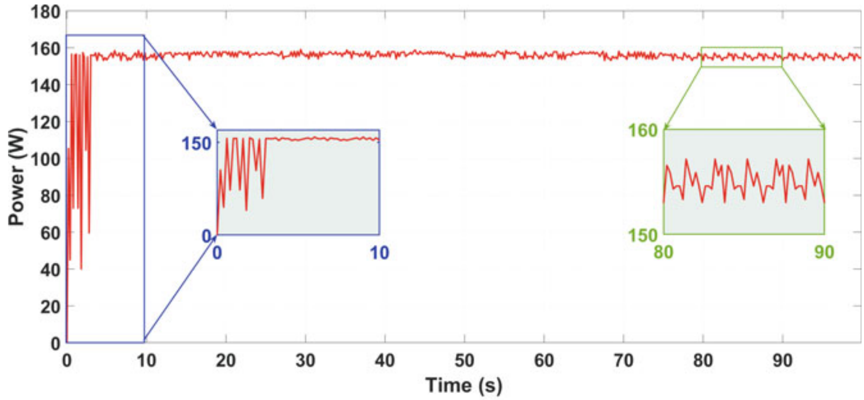

(a)

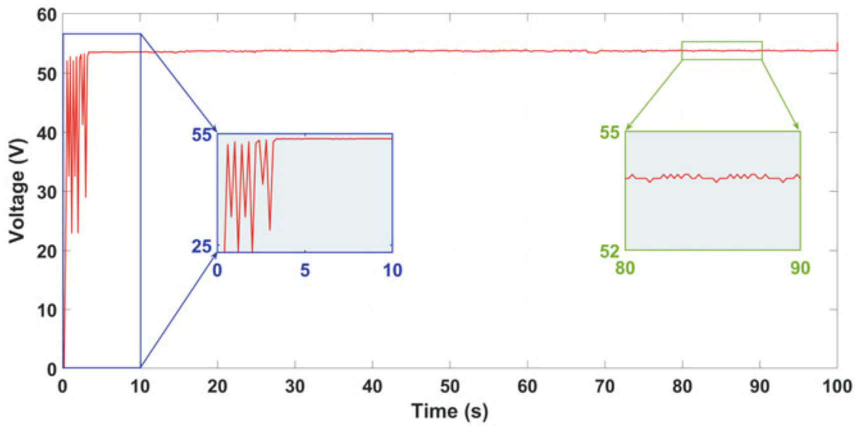

(b)

Fig. 15 Experimental results for the CS algorithm: **a** power and **b** voltage

References

1. Elsakka MM, Ingham DB, Ma L, Pourkashanian M (2021) Comparison of the computational fluid dynamics predictions of vertical axis wind turbine performance against detailed pressure measurements. Int J Renew Energy Res 11:276–293
2. Amer AE, Elsakka MM, Lebedev VA (2021) Thermal performance of an accumulator unit using phase change material with a fixed volume of fins. Int J Energy Res 45:19089–19102. https://doi.org/10.1002/er.7095
3. Abuhashish MN, Daoud AA, Elfar MH (2022) A novel model predictive speed controller for PMSG in wind energy systems. Int J Renew Energy Res 12:170–180. https://doi.org/10.20508/ijrer.v12i1.12750.g8385
4. Elsakka MM, Ingham DB, Ma L, Pourkashanian M (2020) Effects of turbulence modelling on the predictions of the pressure distribution around the wing of a small scale vertical axis wind turbine. In: Proceedings of the 6th European conference on computational mechanics: solids, structures and coupled problems, ECCM 2018 and 7th European conference on computational fluid dynamics, ECFD 2018, pp 3921–3931

5. Osman MH, Seify MAE, Ahmed MK, Korovkin NV, Refaat A (2022) Highly efficient MPP tracker based on adaptive neuro-fuzzy inference system for stand-alone photovoltaic generator system. Int J Renew Energy Res 12:209–217. https://doi.org/10.20508/ijrer.v12i1.12634.g8424
6. Elsakka MM, Ingham DB, Ma L, Pourkashanian M, Moustafa GH, Elhenawy Y (2022) Response surface optimisation of vertical axis wind turbine at low wind speeds. Energy Rep 8:10868–10880. https://doi.org/10.1016/j.egyr.2022.08.222
7. Refaat A, Osman MH, Korovkin NV (2020) Current collector optimizer topology to extract maximum power from non-uniform aged PV array. Energy 116995. https://doi.org/10.1016/j.energy.2020.116995
8. Refaat A, Shehata AA, Elgamal M, Korovkin N V. (2020) Current collector optimizer topology with reconfiguration algorithm to harvest optimal power from nonuniform aged PV arrays. In: 2020 international multi-conference on industrial engineering and modern technologies, FarEastCon 2020, p 9271455
9. Osman MH, Refaat A (2019) Adaptive multi-variable step size P&O MPPT for high tracking-speed and accuracy. IOP Conf Ser Mater Sci Eng
10. Chevtchenko SF, Barbosa EJ, Cavalcanti MC, Azevedo GMS, Ludermir TB (2022) Combining PPO and incremental conductance for MPPT under dynamic shading and temperature. Appl Soft Comput 131:109748. https://doi.org/10.1016/j.asoc.2022.109748
11. Bouarroudj N, Benlahbib B, Sedraoui M, Feliu-Batlle V, Bechouat M, Boukhetala D, Boudjema F (2022) A new tuning rule for stabilized integrator controller to enhance the indirect control of incremental conductance MPPT algorithm: Simulation and practical implementation. Optik (Stuttg) 268:169728. https://doi.org/10.1016/j.ijleo.2022.169728
12. Loukriz A, Haddadi M, Messalti S (2016) Simulation and experimental design of a new advanced variable step size Incremental Conductance MPPT algorithm for PV systems. ISA Trans 62:30–38. https://doi.org/10.1016/j.isatra.2015.08.006
13. Osman MH, Ahmed MK, Refaat A, Korovkin NV (2021) A comparative study of MPPT for PV system based on modified perturbation observation method. In: Proceedings of 2021 IEEE conference Russians young researchers in electrical and electronic engineering, ElConRus 2021, 1023–1026. https://doi.org/10.1109/ElConRus51938.2021.9396444
14. Refaat A, Khalifa A, Elsakka MM, Elhenawy Y, Kalas A, Hegazy M (2023) A novel meta-heuristic MPPT technique based on enhanced autonomous group particle swarm optimization algorithm to track the GMPP under partial shading conditions—experimental validation. Energy Convers Manag 287:117124. https://doi.org/10.1016/j.enconman.2023.117124
15. Refaat A, Kalas A, Khalifa AE, Elfar MH (2023) A comparative study of two metaheuristic MPPT techniques to extract maximum power from PV array under different partial shading patterns. In: IEEE conference on power electronics and renewable energy, CPERE 2023. IEEE
16. Refaat A, Elgamal M, Korovkin NV (2019) A novel photovoltaic current collector optimizer to extract maximum power during partial shading or mismatch conditions. In: Proceedings of the 2019 IEEE conference of Russian young researchers in electrical and electronic engineering, ElConRus 2019, pp 407–412
17. Abouobaida H, Mchaouar Y, Abouelmahjoub Y, Mahmoudi H, Abbou A, Jamil M (2023) Performance optimization of the INC-COND fuzzy MPPT based on a variable step for photovoltaic systems. Optik (Stuttg) 278:170657. https://doi.org/10.1016/j.ijleo.2023.170657
18. Abbass MJ, Lis R, Saleem F (2023) The maximum power point tracking (MPPT) of a partially shaded PV array for optimization using the antlion algorithm. Energies 16:1–13. https://doi.org/10.3390/en16052380
19. Mansoor M, Mirza AF, Ling Q, Javed MY (2020) Novel grass hopper optimization based MPPT of PV systems for complex partial shading conditions. Sol Energy 198:499–518. https://doi.org/10.1016/j.solener.2020.01.070
20. Ahmed J, Salam Z (2014) A maximum power point tracking (MPPT) for PV system using cuckoo search with partial shading capability. Appl Energy 119:118–130. https://doi.org/10.1016/j.apenergy.2013.12.062
21. Hamza Zafar M, Mujeeb Khan N, Feroz Mirza A, Mansoor M, Akhtar N, Usman Qadir M, Ali Khan N, Raza Moosavi SK (2021) A novel meta-heuristic optimization algorithm based

MPPT control technique for PV systems under complex partial shading condition. Sustain Energy Technol Assessments 47:101367. https://doi.org/10.1016/j.seta.2021.101367
22. da Rocha MV, Sampaio LP, da Silva SAO (2020) Comparative analysis of MPPT algorithms based on Bat algorithm for PV systems under partial shading condition. Sustain Energy Technol Assessments 40:100761. https://doi.org/10.1016/j.seta.2020.100761
23. Mohanty S, Subudhi B, Ray PK (2016) A new MPPT design using grey Wolf optimization technique for photovoltaic system under partial shading conditions. IEEE Trans Sustain Energy 7:181–188. https://doi.org/10.1109/TSTE.2015.2482120
24. Chandrasekaran K, Sankar S, Banumalar K (2020) Partial shading detection for PV arrays in a maximum power tracking system using the sine-cosine algorithm. Energy Sustain Dev 55:105–121. https://doi.org/10.1016/j.esd.2020.01.007
25. Azli H, Titri S, Larbes C, Kaced K, Femmam K (2022) Novel yellow saddle goatfish algorithm for improving performance and efficiency of PV system under partial shading conditions. Sol Energy 247:295–307. https://doi.org/10.1016/j.solener.2022.10.029
26. Abo-Khalil AG, Alharbi W, Al-Qawasmi AR, Alobaid M, Alarifi IM (2021) Maximum power point tracking of PV systems under partial shading conditions based on opposition-based learning firefly algorithm. Sustainability 13:1–18. https://doi.org/10.3390/su13052656
27. Aouchiche N, Aitcheikh MS, Becherif M, Ebrahim MA (2018) AI-based global MPPT for partial shaded grid connected PV plant via MFO approach. Sol Energy 171:593–603. https://doi.org/10.1016/j.solener.2018.06.109
28. Mendez-Flores E, Ortiz A, Macias I, Molina A (2022) Experimental validation of an enhanced MPPT algorithm and an optimal DC–DC converter design powered by metaheuristic optimization for PV systems. Energies 15:8043
29. Khalifa AE, Refaat A, Kalas A, Elfar MH (2022) Two bio-inspired MPPT algorithms to harvest the maximum power from partially shaded PV arrays. In: Proceedings of the 2022 conference of russian young researchers in electrical and electronic engineering, ElConRus 2022, pp 670–674
30. Mirza AF, Mansoor M, Ling Q (2020) A novel MPPT technique based on Henry gas solubility optimization. Energy Convers Manag 225:113409. https://doi.org/10.1016/j.enconman.2020.113409
31. Mansoor M, Mirza AF, Ling Q (2020) Harris hawk optimization-based MPPT control for PV systems under partial shading conditions. J Clean Prod 274:122857. https://doi.org/10.1016/j.jclepro.2020.122857
32. Chai LGK, Gopal L, Juwono FH, Chiong CWR, Ling HC, Basuki TA (2021) A novel global MPPT technique using improved PS-FW algorithm for PV system under partial shading conditions. Energy Convers Manag 246:114639. https://doi.org/10.1016/j.enconman.2021.114639
33. Mirza AF, Mansoor M, Ling Q, Yin B, Javed MY (2020) A salp-swarm optimization based MPPT technique for harvesting maximum energy from PV systems under partial shading conditions. Energy Convers Manag 209:112625. https://doi.org/10.1016/j.enconman.2020.112625
34. Gong L, Hou G, Huang C (2022) A two-stage MPPT controller for PV system based on the improved artificial bee colony and simultaneous heat transfer search algorithm. ISA Trans 132:428–443. https://doi.org/10.1016/j.isatra.2022.06.005
35. Zafar MH, Al-Shahrani T, Khan NM, Mirza AF, Mansoor M, Qadir MU, Khan MI, Naqvi RA (2020) Group teaching optimization algorithm based mppt control of pv systems under partial shading and complex partial shading. Electronics 9:1–24. https://doi.org/10.3390/electronics9111962
36. Vamsi Krishna Reddy AK, Venkata Lakshmi Narayana K (2022) Investigation of a social group assisted differential evolution for the optimal PV parameter extraction of standard and modified diode models. Energy Convers Manag 268:115955. https://doi.org/10.1016/j.enconman.2022.115955
37. Elbaz A, Elfar MH, Kalas A, Refaat A (2022) Maximum power extraction from polymer electrolyte membrane (PEM) fuel cell based on deterministic particle swarm optimization algorithm. In: Proceedings of the 2022 conference of Russian young researchers in electrical and electronic engineering, ElConRus 2022, pp 613–619

38. Shehata AA, Refaat A, Ahmed MK, Korovkin NV (2021) Optimal placement and sizing of FACTS devices based on autonomous groups particle swarm optimization technique. Arch Electr Eng 70:161–172. https://doi.org/10.24425/aee.2021.136059
39. Mirjalili S, Lewis A, Sadiq AS (2014) Autonomous particles groups for particle swarm optimization. Arab J Sci Eng 39:4683–4697. https://doi.org/10.1007/s13369-014-1156-x
40. Yang XS, Deb S (2009) Cuckoo search via Lévy flights. In: 2009 world congress on nature and biologically inspired computing, NABIC 2009—proceedings. IEEE, pp 210–214